Double diffraction in an atomic gravimeter

N. Malossi, Q. Bodart, S. Merlet, T. Lévèque, A. Landragin, and F. Pereira Dos Santos*
LNE-SYRTE, Observatoire de Paris, CNRS, UPMC, 61 Avenue de l'Observatoire, F-75014 Paris, France
(Received 28 August 2009; revised manuscript received 19 November 2009; published 20 January 2010)

We demonstrate the realization of a scheme for cold-atom gravimetry based on the recently demonstrated use of double-diffraction beam splitters [T. Lévèque, A. Gauguet, F. Michaud, F. Pereira Dos Santos, and A. Landragin, Phys. Rev. Lett. **103**, 080405 (2009)], where the use of two retro-reflected Raman beams allows symmetric diffraction in $\pm\hbar k_{\mathrm{eff}}$ momenta. Although in principle restricted to the case of zero Doppler shift, for which the two pairs of Raman beams are simultaneously resonant, such diffraction pulses can remain efficient on atoms with nonzero velocity, such as in a gravimeter, when the frequency of one of the two Raman laser sources is modulated. Such pulses are used to realize an interferometer insensitive to laser phase noise and some of the dominant systematics. This approach reduces the technical requirements and would allow the realization of a simple atomic gravimeter. A sensitivity of $1.2 \times 10^{-7} g$ per shot is demonstrated.

DOI: 10.1103/PhysRevA.81.013617 PACS number(s): 03.75.Dg, 37.10.Vz, 37.25.+k, 06.30.Gv

I. INTRODUCTION

Over the past decade, atom interferometry has been increasingly applied to the inertial sensor domain so that state-of-the-art atom gravimeters have reached sensitivities comparable to commercial ones [1,2]. The number of possible applications of gravimetry, ranging from fundamental physics [3,4], metrology [5,6], and geophysics to industrial-related applications, such as navigation and underground prospection, have stimulated research toward higher sensitivity, stability, and overall performance of atomic inertial sensors and toward more compact and movable systems. The present experimental setup, exploiting an atomic interferometer with Raman transitions [7], was originally developed as a prototype for the French watt balance experiment [5], aiming for both high accuracy and discrete portability (interferometer interaction length of a few centimeters only) which, on the other hand, reduces the sensitivity of the interferometer by limiting the interaction time.

A possible solution for increasing the sensitivity of the interferometers is to increase the separation between the atomic wave packets leaving the first beam splitter of the interferometer, thus enlarging the separation of the arms. Material gratings [8], magneto-optical beam splitters [9,10], momentum transfer by adiabatic passage [11], Kapitza-Dirac [12] and Bragg diffraction [13,14] with recent development [15], Bloch oscillations [16,17], and finally Doppler-free double diffraction in Raman configuration [18] have been implemented for obtaining a coherently larger separation angle of the atomic wave packets.

This article shows how the double diffraction scheme described in [18] can be extended to the case of an atomic gravimeter, despite the increasing Doppler shift due to gravity. This scheme essentially consists of the transfer of the same amount of photon momentum $2\hbar k$ in opposite directions from the Raman lasers to both arms of the interferometer, where k is the wave vector of the Raman lasers. This doubles the separation between the atomic wave packets with respect to the usual configuration of an interferometer based on Raman transitions [7] where only one arm gains the momentum transfer. It thus allows an increase in both the intrinsic sensitivity of the interferometer and, thus, the sensitivity to g when the interferometer phase noise is limited by the detection noise or the electronic phase noise of the Raman laser phase difference. When the interferometer noise is dominated by parasitic vibrations, no gain in sensitivity to g is expected. Another advantage of this scheme is to relax the requirements on subsystems such as the phase noise of the microwave reference or the efficiency of magnetic shielding.

II. DOUBLE DIFFRACTION

The Raman transitions couple the two hyperfine ground states of ^{87}Rb atoms ($|g\rangle$ and $|e\rangle$) by using two lasers with frequencies (labeled ω_1 and ω_2) that are detuned to the red of the D_2 line so that the frequency difference between the lasers matches the hyperfine transition frequency.

In this experiment, the two Raman beams are overlapped on a polarizing beam splitter with orthogonal linear polarizations and are injected in the same polarization-maintaining fiber to be sent to the vacuum chamber. At the output of the fiber, the beams pass through a quarter-wave plate, which turns the two polarizations into opposite circular polarizations. These beams are then finally retro-reflected after passing through a second quarter-wave plate. For the two-photon transitions $|F = 2, m_F = 0\rangle \rightarrow |F = 1, m_F = 0\rangle$, there are thus two pairs of beams (with polarizations σ^+, σ^+ and σ^-, σ^-) which can drive the counterpropagating Raman transitions with effective wave vectors $\pm\mathbf{k}_{\mathrm{eff}} = \pm(\mathbf{k}_1 - \mathbf{k}_2)$. The ground state $|g, \mathbf{p}\rangle$ is thus coupled to $|e, \mathbf{p} + \hbar\mathbf{k}_{\mathrm{eff}}\rangle$ by one of the pairs and to $|e, \mathbf{p} - \hbar\mathbf{k}_{\mathrm{eff}}\rangle$ by the other pair.

In the absence of Doppler shift, both pairs are simultaneously resonant so that the atomic population is diffracted into two states $|e, \mathbf{p} \pm \hbar\mathbf{k}_{\mathrm{eff}}\rangle$. This degeneracy was recently used to realize an interferometer for which the difference between the momenta in the two arms is $2\hbar\mathbf{k}_{\mathrm{eff}}$. This scheme increases the inertial sensitivity by a factor of 2 and can be combined with extra Raman pulses to further increase the area of the interferometer [18].

In this article, however, we generalize the previous scheme to atoms with nonzero Doppler shift, allowing the realization

*franck.pereira@obspm.fr

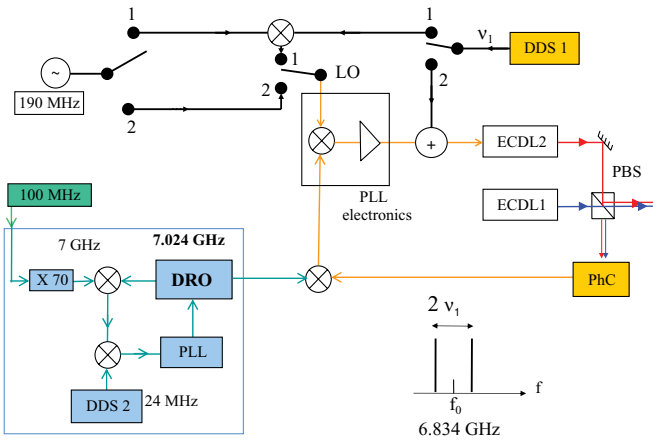

FIG. 1. (Color online) Scheme of the phase-lock loop (PLL). In case 1, the modulation is carried by the local oscillator (LO). In case 2, it is applied directly onto the current of the extended cavity diode laser (ECDL). DRO, dielectric resonator oscillator; PhC, photoconductor.

of an interferometer for gravity measurements. In order to ensure simultaneous resonance with the two transitions while the atoms are free falling, a third frequency is required in the Raman beams. Keeping a two-laser-beam geometry, the three different frequencies can be gained by modulating one of the two lasers to generate sidebands with adjustable separation. Sweeping the modulation frequency allows the resonance condition of the falling atoms to be fulfilled.

Figure 1 displays a scheme of the phase-lock loop (PLL) used to servo the phase difference between the lasers. Modulation of the laser was realized with two different techniques: using a modulated local oscillator (LO) or by adding a modulation on the current of the diode laser. In the first case, the modulated LO is generated by mixing a rf synthesizer at 190 MHz with a direct digital synthesizer (DDS1) whose frequency ν_1 matches the Doppler shift. The LO then contains two frequencies: $190 \pm \nu_1$ MHz. The PLL can efficiently copy the modulated signal onto the frequency difference between the lasers as long as the modulation frequency is smaller than the bandwidth of the PLL (about 4 MHz).

In the second case, the modulation is obtained by directly modulating the current of the diode. Since the PLL effectively works against this modulation, but with a finite gain, an efficient frequency modulation can still be obtained by adjusting the amplitude of the modulation signal. In practice, the modulation amplitude is set to minimize the carrier (more than 40 dB rejection) in order to reduce the influence of parasitic copropagating transitions. Such transitions, although in principle forbidden by polarization selection rules, would still occur due to the relatively small detuning of the carrier (shifted by the recoil frequency ω_R) and imperfections in the polarizations of the Raman beams.

In the standard configuration, the frequency difference between the lasers can then be adjusted at will using either DDS1, which is then used directly as the LO for the phase comparison, or DDS2. In the cases studied here, modifying DDS2 changes the average frequency difference, whereas changing DDS1 modifies the spacing between the sidebands.

A. Experimental setup

The experiment was carried out in the gravimeter setup described in detail in [2,19]. In this compact experimental setup, cold ^{87}Rb atoms are first trapped in a three-dimensional magneto-optical trap (MOT) for a duration of 300 ms. With respect to [2], where a two-dimensional MOT was used, atoms are loaded directly from a background Rb vapor. Atoms are further cooled during a brief optical molasses phase before being released by switching off the cooling lasers. A sequence of microwave and optical pulses is then used to select atoms in the $|F = 2, m_F = 0\rangle$ state. A selection pulse using a standard Raman pulse (diffraction in only one direction) is applied during this sequence in order to reduce the width of the velocity distribution before the atoms experience the interferometer. During their free fall over a few centimeters, the interferometer is obtained by pulsing counterpropagating Raman lasers in the vertical direction. A three-pulse sequence allows splitting, deflection, and recombination of the atomic wave packets. These three successive Raman pulses are separated by the free evolution times of up to $T = 50$ ms. After the interferometer, the populations in the two hyperfine states are measured using a fluorescence detection technique [2].

B. Spectroscopy and Rabi oscillations

As a first step of our investigation, we realize the spectroscopy of the Raman transition. For this measurement, the duration of the selection pulse is set to 120 μs. After the selection, we apply a relatively long single "double-diffraction" Raman pulse of 110 μs, which occurs 17 ms after releasing the atoms from the molasses. The Raman laser intensities are adjusted in order to maximize the transfer efficiency at resonance. Figure 2 displays the measured transition probability as a function of the frequency of DDS2 for three different modulation frequencies: 350, 370, and 375 kHz. At 350 and 370 kHz, two peaks are observed that correspond to individual resonance with one of the two sidebands. For this measurement, the modulation was applied

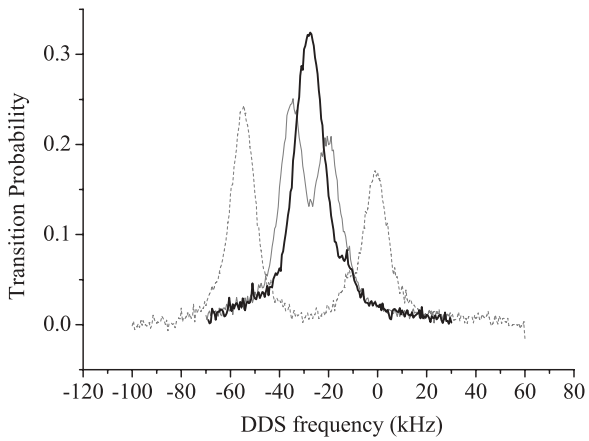

FIG. 2. Raman resonance spectra, obtained by scanning the average Raman frequency DDS2, across the resonance, for three different modulation frequencies: 350 kHz (dashed line), 370 kHz (thin line), and 375 kHz (thick line). At 375 kHz, a single peak is observed, indicating that the two resonance conditions for diffracting up and down are satisfied.

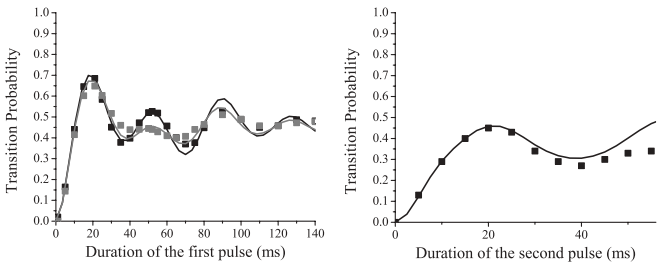

FIG. 3. Transfer efficiency of a double-diffraction pulse. Squares depict measured values and lines are the results of the numerical simulation. Left: first pulse, for atoms selected with standard Raman pulses of duration 23 μs (gray squares and line) and 60 μs (black squares and line). Right: second pulse after a first pulse of duration 18 μs and a pusher beam.

to the diode laser current, which typically results in asymmetric sidebands, as it is evident from the data. This asymmetry results from the cumulative effects of phase and amplitude modulation. At 375 kHz, these two peaks merge, indicating that the two sidebands are simultaneously resonant. Therefore, they are able to diffract atoms in the states $|p \pm \hbar k_{\text{eff}}\rangle$ at the same time.

Having selected the most efficient modulation frequency, 375 kHz, we measured, for atoms that have been velocity selected, the transition probability as a function of the Raman pulse duration at the maximum power available. The left-hand panel of Fig. 3 displays the measurements of the transition probability for two different preselecting Raman transitions of duration 23 and 60 μs (gray and black squares, respectively). A maximum transfer efficiency of about 70% is obtained for a first pulse of duration 18 μs.

After a first pulse of duration 18 μs, atoms left in $|F = 2\rangle$ are cleared by a pulse of a pusher beam, which is tuned on the $|F = 2\rangle \rightarrow |F' = 3\rangle$ transition. A second Raman pulse is then performed, whose transfer efficiency versus duration is plotted in the right-hand panel of Fig. 3.

To discuss the physics of the double-diffraction process, we consider for simplicity the evolution of the quantum state within a three-states basis: $|g, \mathbf{p}\rangle$, $|e, \mathbf{p} + \hbar\mathbf{k}_{\text{eff}}\rangle$, $|e, \mathbf{p} - \hbar\mathbf{k}_{\text{eff}}\rangle$. If the initial state is $|g, \mathbf{p}\rangle$, the transition probability undergoes Rabi oscillations between the two states $|g, \mathbf{p}\rangle$ and $|e, \mathbf{p} + \hbar\mathbf{k}_{\text{eff}}\rangle + |e, \mathbf{p} - \hbar\mathbf{k}_{\text{eff}}\rangle$, with a Rabi frequency Ω_{dd}. An 18-μs-long pulse thus corresponds for our experimental parameters to a π pulse of this oscillation. If now the initial state is $|e, \mathbf{p} + \hbar\mathbf{k}_{\text{eff}}\rangle$, there is a Rabi oscillation between the two states $|e, \mathbf{p} + \hbar\mathbf{k}_{\text{eff}}\rangle$ and $|e, \mathbf{p} - \hbar\mathbf{k}_{\text{eff}}\rangle$ at the frequency $\Omega_{\text{dd}}/2$. With respect to this second Rabi oscillation, the second pulse of the interferometer is a π pulse, whereas it is a 2π pulse with respect the first Rabi oscillation.

In practice, the evolution of the transition probability versus pulse duration is found to differ significantly from the expected sinusoidal dependance of the Rabi oscillations. In particular, the limited efficiency of the second pulse reduces the contrast of the interferometer, which is evident from the data. This deviation from the sinusoidal behavior arises from averaging over the initial vertical velocity distribution, couplings to higher momenta states and spontaneous emission. (The preceding discussion holds only for perfectly resonant plane waves.) We performed the numerical calculation of the evolution of the transition probability, taking into account these effects and extending the basis to the five lowest coupled momenta states. The results of this numerical model are displayed as lines in Fig. 3 for comparison with the experimental data points. The calculations explain the observed behaviors fairly well. In particular, averaging over the initial velocity is the dominant contribution to the imperfection of the double-diffraction pulses.

III. THE INTERFEROMETER

A sequence of three double-diffraction Raman transitions finally allows a double-diffraction interferometer to be realized whose geometry is displayed in Fig. 4. After the first (and eventually the second) pulse, a pulse of pusher beam, resonant with the $|F = 2\rangle \rightarrow |F' = 3\rangle$, clears the atoms in $|F = 2\rangle$. This prevents the formation of parasitic interferometers with the atoms initially left in $|F = 2\rangle$.

The phase of the interferometer can be scanned by changing the chirp rate a applied to DDS1 in order to compensate for the increasing Doppler shift and, thus, to keep the Raman lasers on resonance. Figure 5 displays several interferometer fringe patterns obtained by scanning the chirp rate a, depending on whether a clearing pulse is applied. For this data set, sidebands are produced using a modulated LO and the total interferometer time is set to $2T = 2$ ms. The thick solid line corresponds to the case of a three-pulse interferometer (of durations 18-36-18 μs), with a pulse of pusher beam immediately after the first pulse. As expected for a double-diffraction interferometer, the fringe spacing scales as $2aT^2$. We also checked that the phase of this double-diffraction interferometer is insensitive to a phase jump of the Raman laser

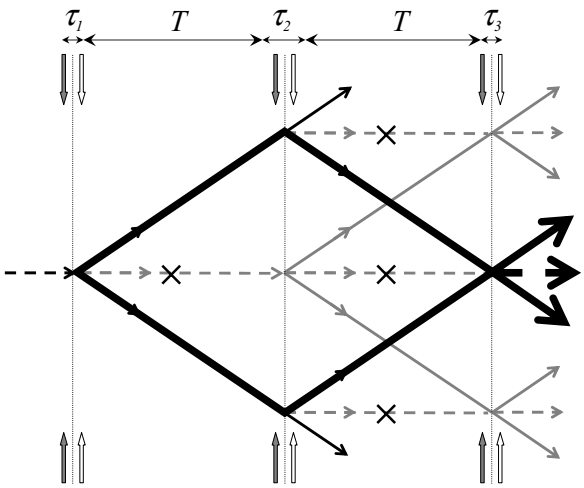

FIG. 4. Scheme of the interferometer, realized with a sequence of three double-diffraction pulses of durations τ_i, separated by free evolutions of duration T. Small arrows represent the retro-reflected Raman lasers. Thick lines represent the two interfering paths that create the double-diffraction interferometer. Thin lines represent parasitic paths, which eventually interfere to create parasitic interferometers. Crosses have been put on the paths removed by pusher beam pulses. Solid (dashed) lines represent partial wave packets in state $|e\rangle$ ($|g\rangle$).

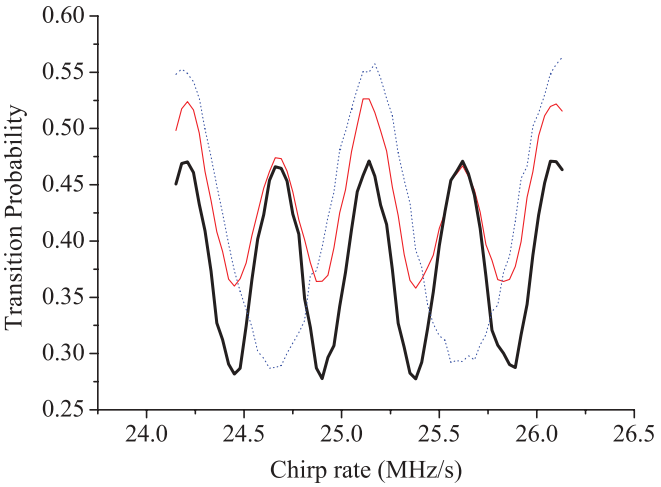

FIG. 5. (Color online) Fringe patterns obtained during modulation of the local oscillator for $2T = 2$ ms: double-diffraction interferometer with pulse sequence 18-36-18 μs (thick solid line), same pulse sequence without pusher pulse (thin solid line), and half-duration Raman pulses (dashed line).

phase difference. The thin solid line corresponds to the same Raman laser pulse sequence, except that the pusher pulse is not used. The fringe pattern exhibits beats between two different fringe spacings, which scale respectively as aT^2 and $2aT^2$. If the pulse durations are reduced by a factor of 2, half-area parasitic interferometers (shown with dashed lines in Fig. 5) dominate the fringe pattern.

The contrast of the interferometer is measured for the two modulation techniques as a function of the interferometer duration $2T$. The results, obtained using two pusher pulses, are displayed in Fig. 6. The contrast is defined here as the difference between the minimum and the maximum of the transition probability. When expressed in percent, it is this difference multiplied by 100. We find a rapid decrease of the contrast with interaction time for the modulated LO case because of the finite bandwidth of the PLL, which is about

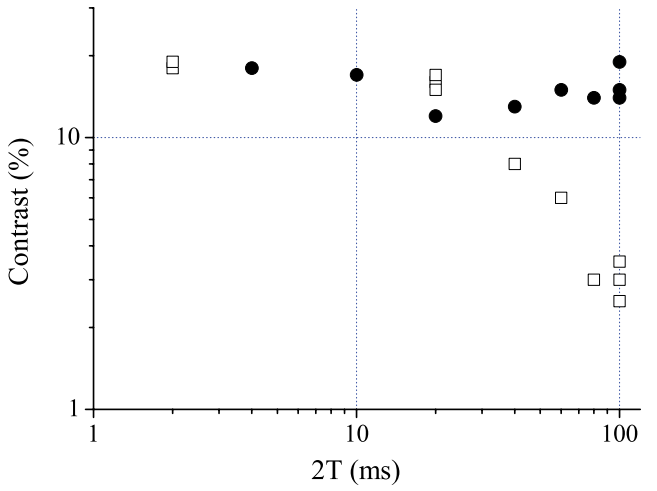

FIG. 6. (Color online) Evolution of the contrast of the interferometer versus total interferometer duration $2T$ for two different techniques: modulated local oscillator (open squares) and modulation of the laser current (solid circles).

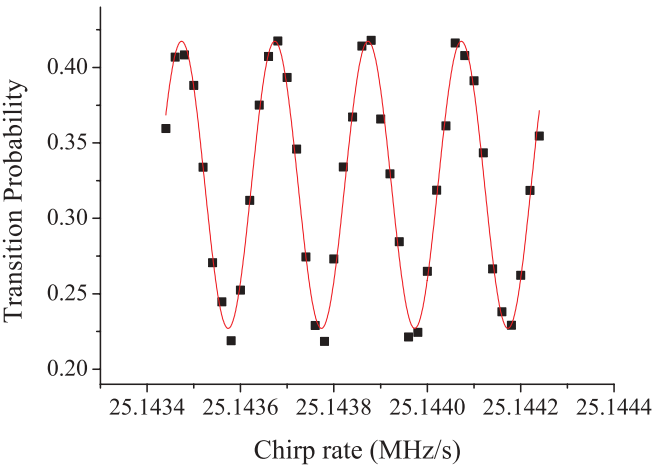

FIG. 7. (Color online) Double-diffraction interferometer fringe pattern, obtained using the current modulation technique, for a total interferometer duration of $2T = 100$ ms.

4 MHz. This decay would be less pronounced if the bandwidth of the PLL was increased, for instance, by using a laser with an intracavity electro-optical modulator (EOM) [20]. In the case where sidebands are produced by modulating the current, the contrast remains almost constant, on the order of 20%. In the latter case, the contrast was found to depend strongly on the operating point of the laser and especially on the tuning sensitivity versus current, which depends on the proximity of mode hops in the laser frequency.

Figure 7 shows an interferometer pattern with $2T = 100$ ms and $\tau = 18$ μs. The contrast is 19%. The number of detected atoms is 2×10^5. The signal-to-noise ratio measured at midfringe is $1/\sigma_{\mathrm{phi}} = 10$, which corresponds to a sensitivity of $1.2 \times 10^{-7} g$ per shot. The influence of residual vibrations is reduced thanks to the combination of a passive isolation platform and a postcorrection scheme using the independent measurement of vibrations with a low noise sismometer [2]. Averaging such a fringe pattern for about an hour allows a high-resolution search for the eventual contribution of a single area parasitic interferometer. Removing the result of a sinusoidal fit with $2aT^2$ scaling reveals well-resolved residuals of aT^2 scaling, whose amplitude is about 1% of the amplitude of the fringes. We believe such parasitic contributions arise from residual copropagating transitions due to imperfect extinction of the carrier.

IV. SYSTEMATICS

In principle, the phase of the interferometer should be insensitive to magnetic field and AC Stark shifts gradients and temporal fluctuations as the two partial wave packets propagate in the same internal state in the two arms of the interferometer. Measurements of the average interferometer phase as a function of the Raman beam intensities are displayed in Fig. 8. The duration of the Raman pulses are adjusted to keep the product $\Omega\tau$ constant. Well-resolved shifts are observed, whose scaling with power does not follow a simple linear dependence. The observed behavior was found to be robust versus changes in the width of the selected velocity class. These phase shifts might be due to the presence of higher-order

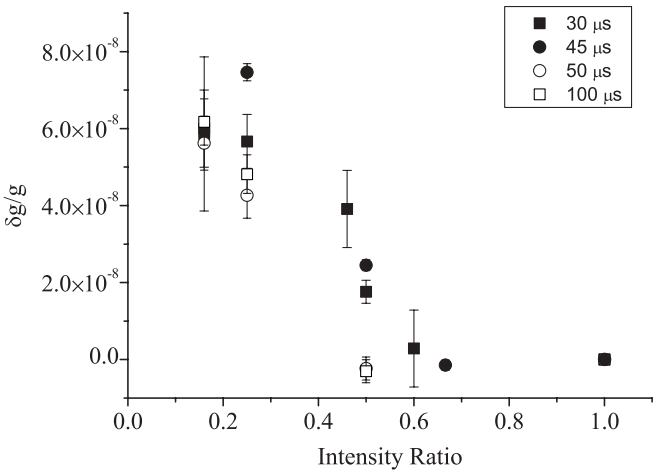

FIG. 8. Relative shift of the interferometer phase as a function of the Raman beam intensity. The intensity is normalized to the maximum intensity available, for which maximum transfer efficiency of a single pulse corresponds to a duration of 18 μs. The different symbols correspond to different durations of the selection pulse.

sidebands, which shift the Raman resonance conditions. A detailed analysis of this effect, which is beyond the scope of this article, deserves further investigation.

V. CONCLUSION

We extend the interferometer scheme based on double diffraction of [18] to the case of a vertical accelerometer. This interferometer geometry results in a factor-of-2 increase of the scale factor and a reduced sensitivity to phase noise and systematics with respect to the traditional geometry. Two different methods are studied, using either a double-frequency LO in the PLL or a modulation of the frequency of one of the two Raman lasers. The best results are obtained with the latter technique, in which the two lowest-order sidebands are used to ensure simultaneous resonance of Raman transitions with effective wave vectors in the up or down directions. This approach allows a good contrast of 19% to be reached for an interferometer of duration $2T = 100$ ms, and a sensitivity of $1.2 \times 10^{-7} g$ per shot for a repetition rate of about 2 Hz. The disadvantages of this last method are parasitic transitions induced by the carrier frequency and light shifts induced by the higher-order sidebands. These drawbacks could be avoided, for instance, by using three independent lasers to generate the three required frequencies. Alternatively, the required frequencies could be obtained by phase modulating a single laser with an EOM, using a two-frequency microwave reference signal. Finally, a further increase of the scale factor can easily be realized with multi-$\hbar k$ beam splitters [18]. Such a geometry, which has increased sensitivity, could allow more compact sensors to be developed, with reduced complexity, as important constraints in the design of the experiment are relaxed by the insensitivity to magnetic field gradients and Raman laser phase noise.

ACKNOWLEDGMENTS

We thank the Institut Francilien pour la Recherche sur les Atomes Froids, the European Union (FINAQS Contract), and the European Science Foundation (EUROQUASAR project) for financial support. Q. B. thanks the Centre National d'Études Spatiales for supporting his work.

[1] A. Peters, K. Y. Chung, and S. Chu, Metrologia **38**, 25 (2001).
[2] J. Le Gouët, T. E. Mehlstäubler, J. Kim, S. Merlet, A. Clairon, A. Landragin, and F. Pereira Dos Santos, Appl. Phys. B **92**, 133 (2008).
[3] J. B. Fixler, G. T. Foster, J. M. McGuirk, and M. A. Kasevich, Science **315**, 74 (2007).
[4] G. Lamporesi, A. Bertoldi, L. Cacciapuoti, M. Prevedelli, and G. M. Tino, Phys. Rev. Lett. **100**, 050801 (2008).
[5] G. Genevès, P. Gournay, A. Gosset, M. Lecollinet, F. Villar, P. Pinot, P. Juncar, A. Clairon, A. Landragin, D. Holleville, F. Pereira Dos Santos, J. David, M. Besbes, F. Alves, L. Chassagne, and S. Topçu, IEEE Trans. Instrum. Meas. **54**, 850 (2005).
[6] S. Merlet, A. Kopaev, M. Diament, G. Geneves, A. Landragin, and F. Pereira Dos Santos, Metrologia **45**, 265 (2008).
[7] M. Kasevich and S. Chu, Phys. Rev. Lett. **67**, 181 (1991).
[8] C. R. Ekstrom, J. Schmiedmayer, M. S. Chapman, T. D. Hammond, and D. E. Pritchard, Phys. Rev. A **51**, 3883 (1995).
[9] T. Pfau, Ch. Kurtsiefer, C. S. Adams, M. Sigel, and J. Mlynek, Phys. Rev. Lett. **71**, 3427 (1993).
[10] T. Schumm *et al.*, Nat. Phys. **1**, 57 (2005).
[11] M. Weitz, B. C. Young, and S. Chu, Phys. Rev. Lett. **73**, 2563 (1994).
[12] S. B. Cahn, A. Kumarakrishnan, U. Shim, T. Sleator, P. R. Berman, and B. Dubetsky, Phys. Rev. Lett. **79**, 784 (1997).
[13] E. M. Rasel, M. K. Oberthaler, H. Batelaan, J. Schmiedmayer, and A. Zeilinger, Phys. Rev. Lett. **75**, 2633 (1995).
[14] D. M. Giltner, R. W. McGowan, and S. A. Lee, Phys. Rev. Lett. **75**, 2638 (1995).
[15] H. Müller, S.-W. Chiow, Q. Long, S. Herrmann, and S. Chu, Phys. Rev. Lett. **100**, 180405 (2008).
[16] P. Cladé, S. Guellati-Khélifa, F. Nez, and F. Biraben, Phys. Rev. Lett. **102**, 240402 (2009).
[17] H. Müller, S.-W. Chiow, S. Herrmann, and S. Chu, Phys. Rev. Lett. **102**, 240403 (2009).
[18] T. Lévèque, A. Gauguet, F. Michaud, F. Pereira Dos Santos, and A. Landragin, Phys. Rev. Lett. **103**, 080405 (2009).
[19] P. Cheinet, F. Pereira Dos Santos, T. Petelski, J. Le Gouët, J. Kim, K. T. Therkildsen, A. Clairon, and A. Landragin, Appl. Phys. B **84**, 643 (2006).
[20] J. Le Gouët, J. Kim, C. Bourassin-Bouchet, M. Lours, A. Landragin, and F. Pereira Dos Santos, Opt. Commun. **282**, 977 (2009).